Author's Accepted Manuscript

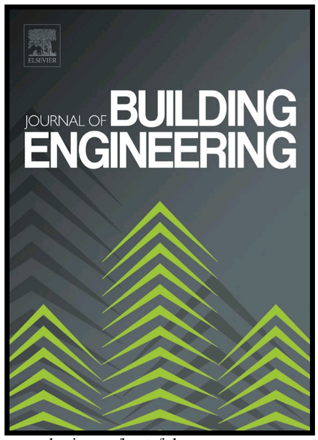

www.elsevier.com/locate/jobe

Flexural Behavior of Self-Compacting Concrete Beams Strengthened with Steel Fiber Reinforcement

H. Mahir Mahmod, Ammar N. Hanoon, Haitham J. Abed

PII: S2352-7102(17)30435-7
DOI: https://doi.org/10.1016/j.jobe.2018.01.006
Reference: JOBE394

To appear in: *Journal of Building Engineering*

Received date: 31 July 2017
Revised date: 10 January 2018
Accepted date: 10 January 2018

Cite this article as: H. Mahir Mahmod, Ammar N. Hanoon and Haitham J. Abed, Flexural Behavior of Self-Compacting Concrete Beams Strengthened with Steel Fiber Reinforcement, *Journal of Building Engineering,* https://doi.org/10.1016/j.jobe.2018.01.006

Flexural Behavior of Self-Compacting Concrete Beams Strengthened with Steel Fiber Reinforcement

H. Mahir Mahmod[1,2,3*], Ammar N. Hanoon[1,3,b], Haitham J. Abed[3,c]
[1] Department of Civil Engineering, Universiti Putra Malaysia, Selangor, Malaysia
[2] Consultant A. Chief Engineer at Ministry of Science and Technology. Baghdad, Iraq
[3] Department of Civil Engineering, Baghdad University, Baghdad, Iraq
mahir.mahmod@gmail.com
civileng.ammar@gmail.com
haithamjameel16@yahoo.com
*Corresponding author: 009647834057225

Abstract
Steel fiber self-compacting concrete (SFSCC) is an innovative material that can flow underneath its own weight in the fresh state, thus eliminating any need for mechanical vibration and complexity of the formwork, and which employs the benefits of steel fibre addition in the hardened state. Hence, this study evaluated the performance of a self-compacting concrete (SCC) under the effect of filler addition and then investigated the effect of steel fiber (SF) addition on flexural behavior, splitting tensile strength, compressive strength, and modulus of elasticity. Fourteen reinforced concrete beams were tested under monotonic loads: two sets of six SCCs (with and without SFs) and two normal concretes (NCs). Ultimate capacity, deflection, crack pattern, and mode of failure were recorded. The present experimental and theoretical results were compared in accordance with ACI 318 codes to assess the applicability of the aforementioned methods to predict the flexural strength of SCC specimens. The results of the tests carried out on fresh concretes indicate excellent deformability without blocking. Moreover, the flexural strength in beams increases with increasing concrete compressive strength, longitudinal steel reinforcement ratio, and SF amount.

Keywords: Concrete structure, failure mode, flexural strength, self-compacting concrete, steel fibers.

List of Symbols

f_y : Yield stress, MPa

f_u : Ultimate stress, MPa

E_c : Modulus of elasticity, MPa

E_{exp} : Experimental modulus of elasticity, MPa

f_{cu} : Ultimate compressive Strength, MPa

f_c' : Compressive strength, MPa

f_t : Splitting tensile strength, MPa

f_r : Modulus of rupture (Flexural Strength of Concrete), MPa

f_{ct} : Compressive strength of tested mixtures, MPa

P_{cr} : Cracking load, KN

P_u : Ultimate load, KN

D_f : Fiber diameter

L_f : Fiber length, mm

V_f : Fiber volume fraction

V_m : Volume fraction of the matrix= 1- V_f

SF : Steel fiber

SCC : Self-compacting concrete

SFSCC : Steel fiber Self-compacting concrete

NC : Normal concrete

RC : Reinforced Concrete

SP : Super plasticizer

LSP : Limestone powder

BR : Blocking ratio

SD : Standard of deviation

C.O.V. : Coefficient of variation

λ : Modification factor

1 Introduction

Self-compacting concrete (SCC) is an important development in concrete technology over the last decades (Adjrad et al., 2016; Biolzi et al., 2014; Ghavidel et al., 2015; Madandoust et al., 2015; Shi et al., 2015; Tichko et al., 2015). SCC may be defined as a concrete that flows under its own weight without the need to any vibration for placing and compaction in the presence of congested reinforcement (Cattaneo & Mola, 2011; Gensel et al., 2011; Goel et al., 2012; Hassan et al., 2010; Shi et al., 2015; Tichko et al., 2015). SCC was first developed in 1986 by Okamura (Oliveira et al., 2015). This technology is considered a vital solution to get a concrete that can flow under its own weight without needing any mechanical vibration and complexity of the formwork. Given its wide applicability, SCC has been explored for its potential in building construction and structural works in numerous countries, such as Japan, Canada, and the United States of America (M. M. Kamal et al., 2014; Oliveira et al., 2015). SCC has many advantages, including high productivity, simple production, and high structure quality (M. Kamal et al., 2017).

Steel fiber self-compacting concrete (SFSCC) mixture shows an improved performance in the fresh and hardened states compared with normal vibrated concrete because of the adding of the fibers (Grünewald & Walraven, 2001). SF addition in concrete mixtures is a nonconventional mass reinforcement that improves the mechanical properties of concrete, ductility, toughness and offers crack propagation control (Dinh et al., 2016; Fritih et al., 2013; Goel & Singh, 2014; Grünewald & Walraven, 2001; Hwang et al., 2016; Islam & Alam, 2013; Tadepalli et al., 2015; Woo et al., 2014). These effects are attributed to the tensile stress transfer capability of SFs across crack surfaces, which is known as crack bridging, and also to the fact that such fibers provide significant resistance to shear across developed cracks. Cracking of SFRC is associated with debonding and pulling out of randomly distributed SFs in concrete. Therefore, SFSCC demonstrates a pseudo-ductile tensile response and enhanced energy dissipation capacities relative to the brittle behavior of plain concrete (Ghavidel et al., 2015). Fritih *et al.* (2013) studied the effect of stainless SFs (0.25% by volume) on the flexural and shear behavior of SCC beams with different ratios of steel reinforcement and reported that the crack width in RC elements in offensive environments can be controlled by adding stainless SF in accordance with the limitations applied by design codes, such as the European code Eurocode 2.

The main parameters that influence flexural behaviors are flexural reinforcement, concrete compressive strength, load conditions, cross-section shape, shear span/depth ratio, and concrete mix design (Jabbar et al., 2016; Mahmod et al., 2017; Sardar et al.). Many techniques have been recently proposed to improve the properties of concrete such as SCC. SCC can flow under its own weight and fill molds easily. Moreover, SCC is a dense and homogeneous material that does not require compaction in narrow areas, such as dense reinforcement (Kanellopoulos et al., 2012). Nonetheless, the mechanical properties of SCC, such as bond, shear, and flexural behavior, are rarely studied despite the extensive research on its fresh properties and durability behavior. Given the lack of information regarding the structural performance of SCC members, designers and engineers in the construction industry do not confidently utilize this material. Thus, the current study focuses on the flexural failure of different grades of reinforced SCC beams (with and without SFs). Woo *et al.* (2014) observed that the flexural tensile strength of SFRC linearly increases as the fiber content increases from 0.87% to 2.61% and the rule of mixture can be applied to SFRC.

The present study demonstrates the results of an experimental study on the flexural behavior of SCC beams with and without SF reinforcements. Test parameters include concrete type, SFs, and flexural reinforcement ratio. The flexural strength, crack patterns, and failure modes of the experimental SCC beams are examined.

2 Experimental program

A total of 14 RC beams with various concrete grades were tested to investigate the flexural failure mechanism and concrete contribution to the overall flexural resistance of SCC beams. These beams were designed for adequate shear reinforcements to study flexural failure. Normal Concrete (NC) and SCC mixtures were used to cast 14 beams with and without fiber reinforcements.

2.1 Beam geometry and reinforcement configuration

The tested beams were divided into three groups according to concrete mix design depending on the type of concrete grade (M_{20}, M_{50} and M_{60}). The total length of each specimen was 1200 mm. The width of all beam specimens was constant at 180 mm, and the overall depth of all beam specimens was 250 mm. Fig. 1, Table 1 and Figure 2 provide the notation utilized to describe each group of test parameters, the details of each specimen**,** and beam geometry with reinforcement distribution respectively. Deformed longitudinal steel bars with nominal diameters of 8, 10, and 16 mm were considered in this study (see Table 2).

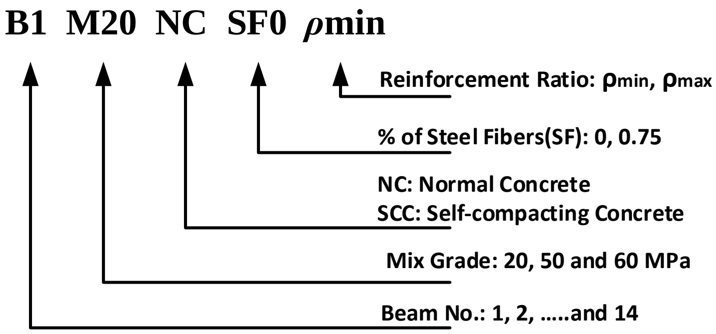

Fig. 1: Notation to indicate the type of each specimen

Table 1: Specimen details

Concrete Grade	Specimen	As (mm^2)	Spacing (mm)
M20	B_1 M_{20} NC SF_0 ρ_{min}	157.00	50
	B_2 M_{20} NC SF_0 ρ_{max}	401.92	30
	B_3 M_{20} SCC SF_0 ρ_{min}	157.00	50
	B_4 M_{20} SCC SF_0 ρ_{max}	401.92	30
	B_5 M_{20} SCC SF_{75} ρ_{min}	157.00	50
	B_6 M_{20} SCC SF_{75} ρ_{max}	401.92	30
M50	B_7 M_{50} SCC SF_0 ρ_{min}	200.96	50
	B_8 M_{50} SCC SF_0 ρ_{max}	803.84	30
	B_9 M_{50} SCC SF_{75} ρ_{min}	200.96	50
	B_{10} M_{50} SCC SF_{75} ρ_{max}	803.84	30
M60	B_{11} M_{60} SCC SF_0 ρ_{min}	200.96	50
	B_{12} M_{60} SCC SF_0 ρ_{max}	1205.80	30
	B_{13} M_{60} SCC SF_{75} ρ_{min}	200.96	50
	B_{14} M_{60} SCC SF_{75} ρ_{max}	1205.80	30

Table 2: Test results of steel reinforcement.

Bar type	Bar diameter, (mm)	Sectional Area, (mm^2)	Yield Stress, f_y (MPa)	Ultimate Stress, f_u (MPa)	Modulus of Elasticity, E_c (Gpa)
Steel	8	50.28	400	472	200
Steel	10	78.57	421	510	200
Steel	16	201.0	552	645	200

Note that each value is an average of three specimens (40 cm length each)

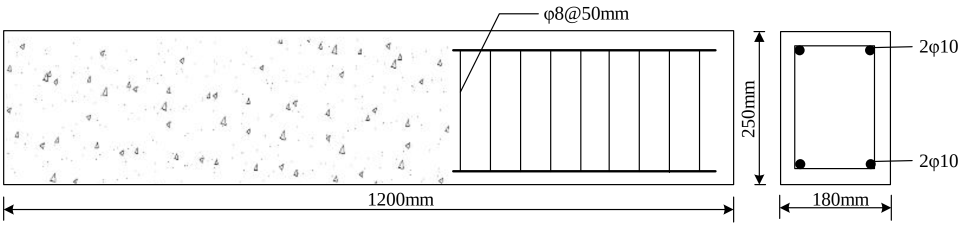

(a) Min reinforcement steel (ρ_{min}) with 50mm spacing (B_1, B_3, B_5, B_7, B_9, $B_{11}$and B_{13})

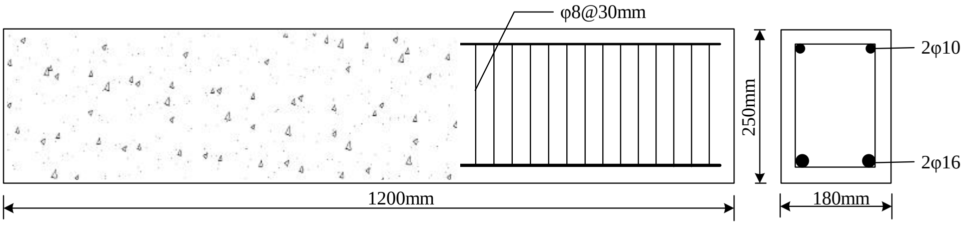

(b) Max reinforcement steel (ρ_{max}) with 30mm spacing (B_2, B_4, B_6, B_8, B_{10}, $B_{12}$and B_{14})

Figure 2: Beam geometry and reinforcement distribution

2.2 Concrete mix design

SCC and NC mixtures were utilized to cast 14 RC beams, 21 cubes (150×150) mm, 21 prisms (100× 100 × 500) mm and 63 cylinders (150×300) mm, to investigate flexural, compressive strength, split, and modulus of elasticity (Fig. 3). Two sets of SCC mixtures with and without SF and one NC mixture were manufactured in the laboratory.

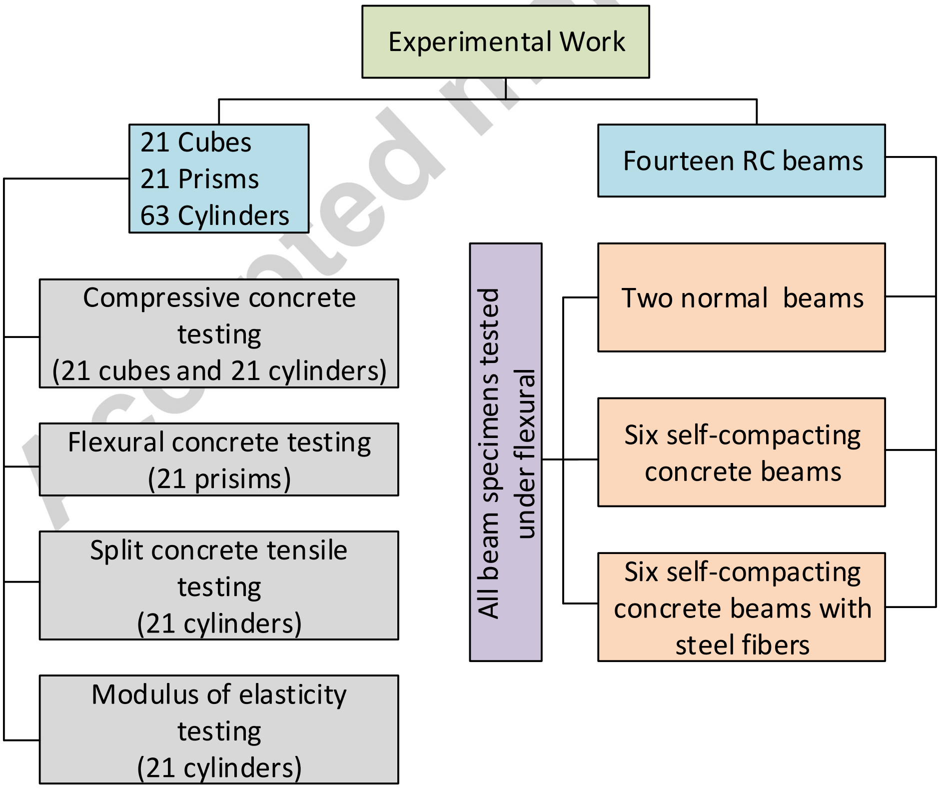

Fig. 3: Experimental work program

The properties of the two sets of SCC and NC mixtures are listed in Table 3, where M_{20}SCC, M_{50}SCC, and M_{60}SCC are the SCC mixtures and M_{20}NC is the NC mixture. The cement contents in these three mixes were unequal, and each mix was designed to contain cement for the development of concrete compressive strength. The NC mixture was selected as the reference in both fresh and hardened states to evaluate the performance of SCCs with and without SF.

Table 3: Properties of the self-compacting concrete (SCC) and normal concrete (NC)

Mixture	Cement (Kg/m^3)	Sand (Kg/m^3)	Gravel (Kg/m^3)	Water (litter/m^3)	SP	LSP (Kg/m^3)	Total (Cement +LSP)	W/Total
M_{20}SCC SF0	270	780	850	187	6.5	250	520	0.35
M_{50}SCC SF0	500	785	850	173	8.5	85	585	0.29
M_{60}SCC SF0	550	825	850	150	12	50	600	0.25
M_{20}SCC SF75	270	780	850	187	9	250	520	0.35
M_{50}SCC SF75	500	785	850	173	11	85	585	0.29
M_{60}SCC SF75	550	825	850	150	15	50	600	0.25
M_{20}NC	300	600	1100	180	-	-	-	0.60

Table 4 shows the physical properties of the ordinary Portland ASTM Type I cement used in this study. The fine aggregate utilized was a local natural sand with a specific gravity, water absorption, and sulfate content of 2.6, 0.75%, and 0.11%, respectively. Crushed gravel was used as coarse aggregate; the particles had a maximum size, specific gravity, water absorption, and sulfate content of 10 mm, 2.6, 0.75%, and 0.061%, respectively.

Table 4: Physical properties of cement

Physical properties	Test result
Specific surface area (Blaine Method), m^2/kg	333
Setting time (Yicale's method)	
Initial setting, hrs: min	2.00
Final setting, hrs: min	4.10
Compressive strength, MPa	
3 days	16.2
7 days	24.1
Autoclave expansion %	0.25

A polycarboxylic super plasticizer was applied as admixture for all tested SCCs. This plasticizer, which is known commercially as "GLENIUM51", had a specific gravity and relative density of 1.21 and 1.1, respectively. This SP is chloride free and complies with (ASTM-C494M, 2011) types A and F; Table 5 shows its physical properties.

Table 5: Physical properties of "GLENIUM51"

Main action	Concrete super plasticizer

Form	Viscous fluid
Appearance	Light brown
Density	1.1 g/cm^3 @ 20C°
pH value	6.6
Viscosity	128+/-30 cps @ 20 C°
Labeling	No hazard label required

Fine limestone powder (LSP) with a fineness of 3100 gm/cm² was used as an additive to avoid excessive heat generation, enhance fluidity and cohesiveness, improve segregation resistance, and increase the amount of fine powder in the mixture (cement and filler). Table 6 lists the chemical composition of LSP.

Table 6: Chemical composition of limestone powder

Oxides	%
Calcium oxides Cao	54.1
Silicon oxides SiO2	1.28
Aluminum oxides Al2O3	0.72
Ferric oxides Fe2O3	0.12
Magnesium oxides MgO	0.13
Sluphur trioxides SO3	0.21
Loss on Ignition L.O.L	42.56

Waved (or crimped) SFs with a volume fraction (V_f) of 0.75% were used. This SF volume represents a typical value and is used in several experimental investigations. Table 7 summarizes the properties of the SF material.

Table 7: Steel fiber properties

Type	Waved (or Crimped)
Density (Kg/m^3)	7860
Ultimate Strength (MPa)	1500
Possion's Ratio	0.28
Length (mm)	32
Diameter (mm)	0.4
Aspect	80
Modulus of Elasticity (MPa)	200000

2.3 Mixing procedure

Both SCC and NC mixtures were mixed by using a rotary mixer with a 0.19 m^3 capacity. Tests were conducted on the fresh properties of the SCC mixtures immediately after mixing concluding slump and L-box tests in accordance with (BS-EN-12350-8, 2010; BS-EN-12350, 2010), respectively. L-box test was used to assess the filling and passing ability of SCC or the ability of concrete to pass though reinforced bars without blocking or segregation. The steps of the fresh test are detailed in Fig. 4.

Fig. 4: Experimental tests for fresh properties of self-compacting concrete (SCC)

2.4 Experimental setup, instrumentation, and test observations

The instrumentation for the beam test program included a load cell, strain gauges, and a linear variable displacement transducer. A hydraulic universal testing machine (MFL system) with a 3000 kN capacity was attached to the actuator to measure load (Fig. 5). The formworks were removed after 1 day of casting, and specimens were cured in a humidity chamber for approximately 24 days. These specimens were then removed from the chamber 3 days before testing.

Beam specimens were tested as simply supported beams under a four-point load condition. Fig. 6 displays the schematic of the test setup. The initiation and development of cracks and cracking loads at various levels were recorded during loading time. The tests also obtained information on the overall behavior of beams, including failure modes and influence of concrete characteristics. Loading was maintained until the beams failed.

Fig. 5: Hydraulic universal testing machine (MFL system) used to test the beams

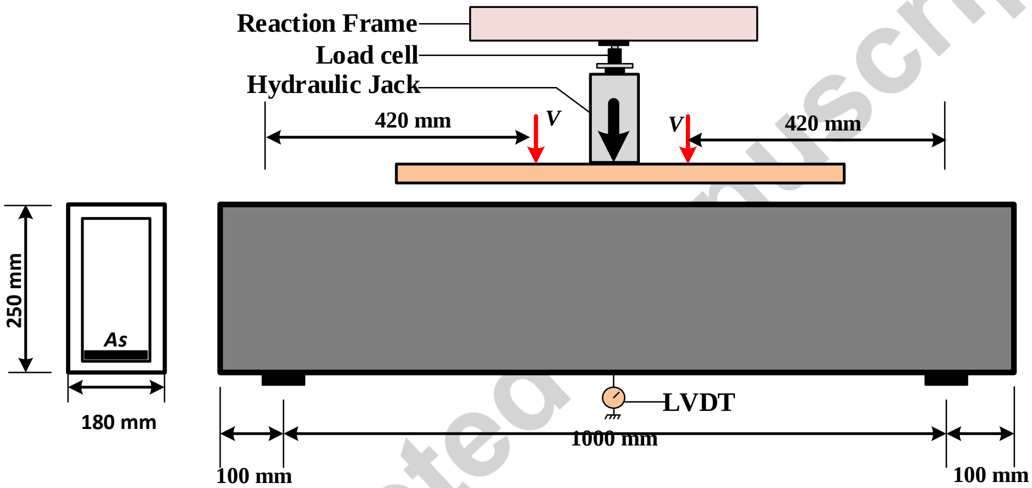

Fig. 6: Schematic of the experimental set-up

3 Results and Discussion

3.1 Fresh concrete properties

3.1.1 Slump test

Table 8 illustrates the results of the fresh concrete property test with and without SFs. The (*D*) values represent the maximum spread slump flow final diameter, and the T50 values represent the time required for the concrete flow to reach a circle with a 50 cm diameter. These results are within the acceptable criteria for SCC given by (ACI-363, 2010) and indicate excellent deformability without blocking.

3.1.2 L-box test

L-box results are listed in Table 8. The blocking ratio (BR) values exceeded 0.80, which is often considered a critical lower limit (ACI-363, 2010). The results indicate favorable deformability without blocking through closely spaced obstacles and the good ability of the highly flowable SCC.

Table 8: Test results of fresh concrete properties (with and without SF)

Mix	Slump Flow (D) (mm)		Slump Flow (T50) (Sec)		L - Box (BR) (%)		L-Box (T20) (Sec)		L-Box (T50) (Sec)	
	SF_{75}	SF_0	SF_{75}	SF_0	SF_{75}	SF_0	SF_{75}	SF_0	SF_{75}	SF_0
M_{20}SCC	655	705	4.5	1.8	0.8	0.89	2.5	1.3	4.7	3.2
M_{50}SCC	663	750	4.93	3.3	0.85	0.91	3.4	1.5	5.9	3.3
M_{60}SCC	692	780	5	3.97	0.88	0.95	3.8	2.5	7.1	4.45

3.2 Hardened concrete properties

3.2.1 Compressive strength

Table 9 presents the experimental values of concrete compressive strength which was carried out in accordance with (ASTM-C39M, 2012). Test results showed that SF addition improved compressive strength values by 20%–38% in normal strength concrete (NSC). In addition, the presence of SFs altered the failure mode of concrete specimens from a brittle to a ductile failure. This improvement is due to the confinement of the fiber reinforcement on the specimen, this confinement is able to reduce transversal deformation of specimen and increase its compressive strength. In addition, the most important effect of steel fibers is prevention of crack propagation in concrete. Thus, extension and propagation of micro cracks that occur due to internal stress in concrete are prevented by stress transfer capability of fibers. The general configuration of the tested specimens was maintained as the original after failure.

Table 9: Compressive strength of tested mixtures, MPa

Mix	f_{cu} (MPa)	f_c' (MPa)	f_{cu} / f_c'	f_{ct} (MPa)	f_r (MPa)	E_c (MPa)
M_{20} NC	19.11	16.99	0.88	2.40	4.50	13480.35
M_{20} SCC SF_0	24.00	20.38	0.84	2.61	6.75	14696.02
M_{20} SCC SF_{75}	29.10	23.50	0.80	3.75	9.90	18082.28
M_{50} SCC SF_0	49.03	39.34	0.80	5.37	11.34	24150.15
M_{50} SCC SF_{75}	55.85	48.12	0.86	6.65	14.12	26927.33
M_{60} SCC SF_0	61.40	55.20	0.89	7.92	15.89	25986.55
M_{60} SCLC SF_{75}	68.74	61.88	0.90	9.05	17.55	30214.05

3.2.2 Splitting tensile strength (f_t)

Splitting tensile strength test was performed in accordance with as described in (ACI-318M, 2014) and (ACI-363, 2010), hTable 10 presents the splitting tensile strength for different concrete types. Both measured and calculated results provided approximately close values.

hTable 10: Splitting tensile strength of tested specimens, MPa

Concrete Type	f_c' (MPa)	f_t (MPa)		Notes
		Experimental (average of three samples)	ACI	
M_{20} NC	16.99	2.406	2.06	ACI-318, ($0.5\sqrt{f_c'}$)
M_{20} SCC SF_0	20.38	2.618	2.26	ACI-318, ($0.5\sqrt{f_c'}$)
M_{20} SCC SF_{75}	23.50	3.75	-	Not Covered in ACI-544
M_{50} SCC SF_0	39.34	5.378	3.14	ACI-318, ($0.5\sqrt{f_c'}$)
M_{50} SCC SF_{75}	48.12	6.652	-	Not Covered in ACI-544
M_{60} SCC SF_0	55.20	7.926	4.41	ACI-363, ($0.59\sqrt{f_c'}$)
M_{60} SCC SF_{75}	61.88	9.058	-	Not Covered in ACI-544

3.2.3 Modulus of rupture

Modulus of rupture was conducted in accordance with (ASTM-C78M, 2010). Table 11 shows the values of experimental rupture modulus for different concrete types in comparison with the value approximations determined by (ACI-318M, 2014; ACI-363, 2010; ACI-544, 1999).

Table 11: Test results of modulus of rupture, MPa

Concrete Type	f_c' (MPa)	f_r (MPa)		Notes
		Experimental *	ACI	
M_{20}NC	16.99	4.5	2.55	ACI-318, ($0.62\lambda\sqrt{f_c'}$)
M_{20} SCC SF_0	20.38	6.75	2.79	ACI-318, ($0.62\lambda\sqrt{f_c'}$)
M_{20} SCC SF_{75}	23.49	9.9	11.57	ACI-544, ($0.97 f_r V_m + 3.406 V_f \frac{L_f}{D_f}$) **
M_{50} SCC SF_0	39.34	11.34	3.88	ACI-318, ($0.62\lambda\sqrt{f_c'}$)
M_{50} SCC SF_{75}	48.12	14.12	15.64	ACI-544, ($0.97 f_r V_m + 3.406 V_f \frac{L_f}{D_f}$) **
M_{60} SCC SF_0	55.22	15.89	6.98	ACI-363, ($0.94\sqrt{f_c'}$)
M_{60} SCC SF_{75}	61.88	17.55	18.94	ACI-544, ($0.97 f_r V_m + 3.406 V_f \frac{L_f}{D_f}$) **

λ= Modification factor= 1 for Normal weight (See Table 19.2.4.2 ACI 318M-14).

* Average of three samples.

** Converted to SI units.

3.2.4 Modulus of elasticity (E_c)

Table 12 lists the modulus of elasticity for various concrete strengths. The static modulus of elasticity of concrete (E_c) for NC and SCC was measured as described by (Madandoust et al., 2015) and in accordance with (ACI-318M, 2014), (ACI-363, 2010) and (ASTM-C469M, 2010) technique (secant to 0.4 f_c'). Since there is a slight differences in modulus of elasticity of concrete samples with and without SF. It can be clearly seen, from Fig. 7 and Table 12, that the modulus of elasticity of concrete was not significantly affected by the incorporation of SF_{75} for modulus of elasticity obtained experimentally and estimated by ACI. (Gencoglu et al., 2002).

Table 12: Test results of modulus of elasticity (E_c), MPa

Concrete Type	f_c' (MPa)	E_c (MPa)		
		Experimental: average of 3 samples	ACI- Code	
		ASTM-469 Secant to ($0.4 f_c'$)	ACI-318 ($4700\sqrt{f_c'}$)	ACI-363 ($3320\sqrt{f_c'} + 6900$)
M_{20}NC	16.99	13480.35	19370.05	20188.45
M_{20} SCC SF_0	20.38	14696.02	21218.82	22115.34
M_{20} SCC SF_{75}	23.49	18082.28	22782.16	24659.88
M_{50} SCC SF_0	39.34	24150.15	29482.15	30727.81
M_{50} SCC SF_{75}	48.12	26927.34	32604.59	35291.89
M_{60} SCC SF_0	55.22	25986.55	34919.77	31566.73
M_{60} SCC SF_{75}	61.88	30214.05	36972.00	40019.92
SD	-	6500.198	7061.694	7235.634
Mean	-	21933.82	28192.79	29224.29
C.O.V.	-	3.374331	3.992355	4.03894

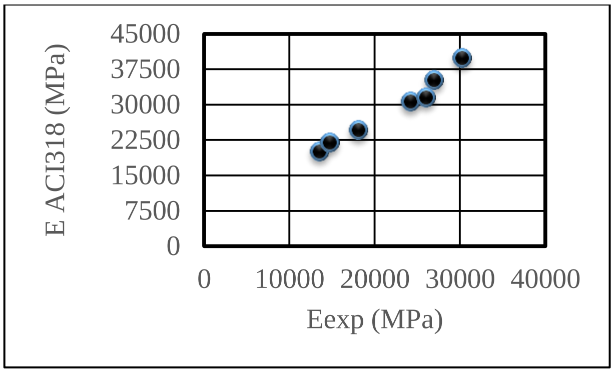

(a)

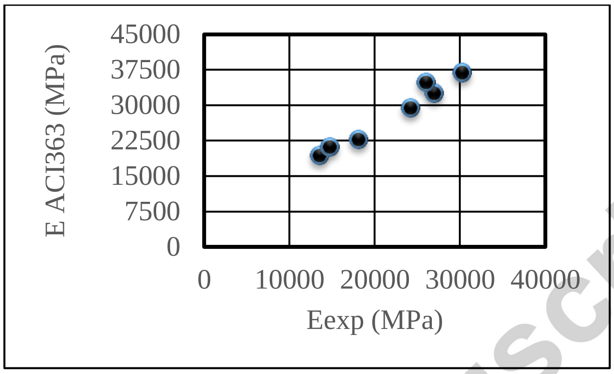

(b)

Fig. 7: Comparison between experimental and predicted modulus of elasticity according to (a) ACI 318 and (b) ACI 363, respectively

3.2.5 Results of bending tests

Fourteen RC beam specimens were tested to evaluate the experimental bending results. Twelve beams were manufactured for SCC: six specimens with 0.75 of SFs and another six without SFs; two beams were casted with NC. For the control beams, important remarks were recorded regarding mixing, pouring, curing, mold stripping, and testing at the early stages of the present work. On the basis of these remarks, modifications in steel mold shape and point load locations were performed.

Table 13 shows the average results of the mechanical tests of the control samples. All results were compared with ACI and can be considered acceptable within the ACI limits.

Table 13: Test results of beam specimens, MPa

	f_c' (MPa)	E_c test (MPa)	f_t (MPa)	E_c ACI (MPa)	E_c test/ E_c ACI	f_t ACI (MPa)	f_t test/ f_t ACI
B_1 M_{20} NC SF_0 ρ_{min} B_2 M_{20} NC SF_0 ρ_{max}	16.99	13480.35	2.40	19370.05	0.69	2.06	1.17
B_3 M_{20} SCC SF_0 ρ_{min} B_4 M_{20} SCC SF_0 ρ_{max}	20.38	14696.02	2.61	21218.82	0.692	2.26	1.16
B_5 M_{20} SCC SF_{75} ρ_{min} B_6 M_{20} SCC SF_{75} ρ_{max}	23.49	18082.28	3.75	22782.16	0.794	Not covered	--
B_7 M_{50} SCC SF_0 ρ_{min} B_8 M_{50} SCC SF_0 ρ_{max}	39.34	24150.15	5.37	29482.15	0.819	3.14	1.71
B_9 M_{50} SCC SF_{75} ρ_{min} B_{10} M_{50} SCC SF_{75} ρ_{max}	48.12	26927.34	6.65	32604.59	0.825	Not covered	--
B_{11} M_{60} SCC SF_0 ρ_{min} B_{12} M_{60} SCC SF_0 ρ_{max}	55.22	25986.55	7.92	34919.77	0.744	4.41	1.80
B_{13} M_{60} SCC SF_{75} ρ_{min} B_{14} M_{60} SCC SF_{75} ρ_{max}	61.88	30214.05	9.05	36972.60	0.817	Not covered	--

3.2.6 Flexural Behavior

Fig. 8 shows the tested beams. All of the beams in this study were designed to fail in flexural with tensile mode, which is characterized by the formation of cracks in the tensile stress zone loaded with point load, subsequently yielding steel bars and shifting the neutral axis toward the compression zone. The main cracks for all tested beams commenced at the middle zone, and all beams exhibited ductile flexural failure (Fig. 9). The behavior of all beam specimens was generally similar up to failure. The addition of SFs to SCC samples enhanced the ultimate capacity of the beams (Pająk & Ponikiewski, 2013). The addition of SFs to B_5 above B_3 and B_1 increased the ultimate capacity Pu of SCC samples by 4.34% and 6.67%, respectively. Similarly, the development for B_6 was approximately 7.69% and 16.67% above B_2 and B_4, respectively.

3.2.7 Ultimate Load and Failure Mode

In all specimens, the first crack was flexural in the maximal moment zone for a load value between 9 and 20 kN. Other flexural cracks occurred at higher loading levels. The crack spacing was lighter while the crack network was denser in the beams with SFs than in the SCC and NC beams. In each group, crack propagation was delayed in the fiber-reinforced beams. This phenomenon can be explained bratioy the capability of the fibers to transfer stresses to the concrete through a crack. Crack distribution was slightly more regular in the fiber-reinforced beams than in the SCC beams. Thus, the contribution of the concrete area between two existing flexural cracks to the tensile strength (i.e., concrete tension stiffening) was enhanced. This technique improved integrated tensile stresses and thus produced new cracks when the concrete tensile strength was reached. The crack density under such conditions increased, a result that can be compared with that under a high longitudinal reinforcement ratio (Abrishami & Mitchell, 1997), which also increases the tensile stress transmission to concrete through the steel–concrete interface.

The cracking, ultimate load, and deflection are presented in Table 14, and the crack patterns for all tested specimens are shown in Fig. 8. Usual flexural and diagonal cracks were encountered in all beams. The first crack loads recorded ranged from approximately 2.65% to 4.58% for all beams.

The ultimate and cracking load carrying capacities of the SCC (with SFs) beams were greater than those of the SCC and NC beams. This result can be attributed to the capability of the SFs to confine crack growth. Additional points can be drawn from the following experimental tests.

As predicted, the main cracks for all tested beams started at the middle zone, and all beams exhibited ductile flexural failure (Fig. 8). Most of the cracks developed at the bottom of the beams at 60% of the ultimate load. Regarding odd beams starting from B_3 with $\rho_{min.}$, the first crack ranged from 11.1% to 100% for. Meanwhile, even beams starting from B_4 with $\rho_{max.}$, the first crack ranged from 5% to 100%/.

Table 14: Cracking load and deflection at ultimate loads, kN

Specimen	Cracking Load, P_{cr} (KN)	Deflection, (m)	Ultimate Load, P_u (KN)	P_{cr} /P_u (%)
B_1 M_{20} NC SF_0 ρ_{min}	9.000	0.0190	225	4.00
B_2 M_{20} NC SF_0 ρ_{max}	10.00	0.0175	240	4.17
B_3 M_{20} SCC SF_0 ρ_{min}	10.00	0.0180	230	4.34
B_4 M_{20} SCC SF_0 ρ_{max}	10.50	0.0160	260	4.04
B_5 M_{20} SCC SF_{75} ρ_{min}	11.00	0.0170	240	4.58
B_6 M_{20} SCC SF_{75} ρ_{max}	11.75	0.0140	280	4.19
B_7 M_{50} SCC SF_0 ρ_{min}	12.00	0.0135	350	3.42
B_8 M_{50} SCC SF_0 ρ_{max}	12.50	0.0110	450	2.80
B_9 M_{50} SCC SF_{75} ρ_{min}	12.75	0.0100	385	3.31

B_{10} M_{50} SCC SF_{75} ρ_{max}	13.00	0.0085	490	2.65
B_{11} M_{60} SCC SF_{0} ρ_{min}	14.50	0.0120	370	3.91
B_{12} M_{60} SCC SF_{0} ρ_{max}	15.00	0.0090	475	3.16
B_{13} M_{60} SCC SF_{75} ρ_{min}	18.00	0.0050	410	4.39
B_{14} M_{60} SCC SF_{75} ρ_{max}	20.00	0.0030	595	3.36
SD	-	-	-	0.140
Mean Value	-	-	-	3.737
C.O.V.	-	-	-	0.164

Cracks are concentrated at middle span

No wide cracks appears as in B_1

Cracks distribution along the beam span

No wide cracks appears as in B_3, cracks at left support are may be due to incorrect sample setting

Contributions of SF_{75} with SCC produce fewer cracks

Using ρ_{max} make sample stiffer than sample B_5

Increasing of f_c'made sample stiffer

Increasing of steel area using ρ_{max} made sample B_8 stiffer than B_7, less cracks width

Cracks concentrated at middle span

Less cracks width compared with B_9, failure at left support may be cause of bad setting of a sample B_{10}

The cracks kept its distribution at middle span

Less crack width since using ρ_{max} compared with B_{11}

Increasing of f_c'and contribution of SF_{75} with SCC cause a reduction in cracks number

Increasing of f_c', ρ_{max} and SF_{75} cause less cracks width

Fig. 8: Test of beams at failure stage

3.2.8 Load Deflection Characteristics

The deflection at mid span of all the three beam groups was recorded every 2 kN load increment (Fig. 9). The deflection at mid span decreased with increasing SF amount; this result can be attributed to the improved flexural stiffness of the beam specimens that reduced beam deformation and subsequently controlled cracking. At the early stages of loading application, no interface slip caused by the increasing cohesion between SFs and concrete was noted.

Before the first crack initiation, the beams behaved similarly in terms of load deflection relationship. At this phase, the evolution of stiffness did not depend on the presence of SFs. All of the beams exhibited a nonlinear response after the first crack appearance.

The tested beams showed an increase in mid span deflection with increasing concrete compressive strength. Meanwhile, the deflection significantly decreased with increasing steel reinforcement ratio in terms of ρ_{max}.

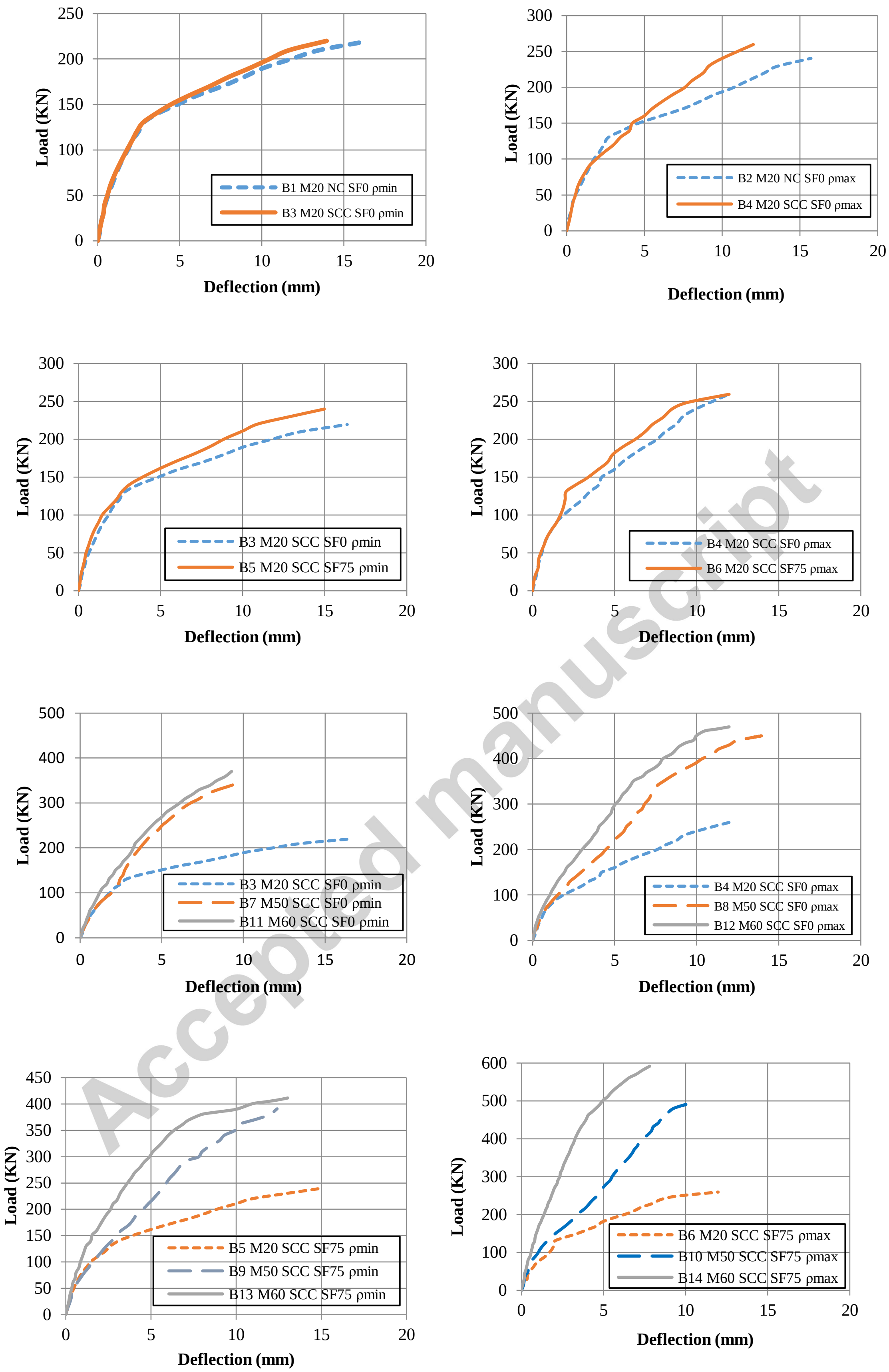

Fig. 9: Load–deflection curves.

4 Conclusions

The effect of using SCC combined with SFs in RC beams was examined and discussed. The following conclusions were obtained:

- SF addition to fresh concrete decreased workability and flowability but improved hardened properties, such as compressive strength and flexural strength because of SF addition.
- An increase in SCC compressive strength from 20.38 MPa to 55.22 MPa improved the cracking load by 45% and about 63.64% for SCC with SF addition.
- The tested SFSCC beams showed more ductile behavior and thus possessed stronger energy absorption than the SCC and NC beams.
- All beam specimens indicated a similar trend of crack spread with concrete crushing near the compression zone.
- The crack width was substantially reduced because of SF confinement.
- All tested beams with SCC decreased in midspan deflection with increasing concrete compressive strength.
- SF addition to SCC is significantly improved the behavior and flexural capacity.

Acknowledgements

The authors would like to express their gratitude to the support provided by Baghdad University, Iraq. The first author gratefully acknowledges the support provided by Ministry of Science and Technology, Baghdad, Iraq.

References

Abrishami, H. H., & Mitchell, D. (1997). Influence of steel fibers on tension stiffening. *Structural Journal, 94*(6), 769-776. doi: 10.14359/9736

ACI-318M. (2014). Metric Building Code Requirements for Structural Concrete and Commentary. Farmington Hills, MI., USA: American Concrete Institute.

ACI-363. (2010). Report on High Strength Concrete Farmington Hills, MI, USA: ACI Committee 363.

ACI-544. (1999). Design Considerations for Steel Fiber Reinforced Concrete (ACI 544.4R-88 (Reapproved 1999)). Farmington Hills, Mich., USA: ACI Committee 544.

Adjrad, A., Bouafia, Y., Kachi, M., & Ghazi, F. (2016). Prediction of the Rupture of Circular Sections of Reinforced Concrete and Fiber Reinforced Concrete. *International Journal of Concrete Structures and Materials*, 1-9. doi: 10.1007/s40069-016-0137-8

ASTM-C39M. (2012). Standard Test Method for Compressive Strength of Cylindrical Concrete Specimens. West Conshohocken, USA: American Society for Testing and Material.

ASTM-C78M. (2010). Standard Test Method for Flexural Strength of Concrete (Using Simple Beam with Third-Point Loading). West Conshohocken, USA: American Society for Testing and Material.

ASTM-C469M. (2010). Standard Test Method for Static Modulus of Elasticity and Poisson's Ratio of Concrete in Compression. West Conshohocken, USA: American Society for Testing and Material.

ASTM-C494M. (2011). Standard Specification for Chemical Admixtures for Concrete. West Conshohocken, USA: American Society for Testing and Material.

Biolzi, L., Cattaneo, S., & Mola, F. (2014). Bending-shear response of self-consolidating and high-performance reinforced concrete beams. *Engineering Structures, 59*, 399-410. doi: 10.1016/j.engstruct.2013.10.043

BS-EN-12350-8. (2010). Testing fresh concrete. Self-compacting concrete. Slump-flow test (pp. 14): BSI.

BS-EN-12350. (2010). Testing fresh concrete. Self-compacting concrete. L box test (pp. 14): BSI.

Cattaneo, S., & Mola, F. (2011). Assessing the quality control of self-consolidating concrete properties. *Journal of Construction Engineering and Management*. doi: 10.1061/(asce)co.1943-7862.0000410

Dinh, N.-H., Choi, K.-K., & Kim, H.-S. (2016). Mechanical Properties and Modeling of Amorphous Metallic Fiber-Reinforced Concrete in Compression. *International Journal of Concrete Structures and Materials*, 1-16. doi: 10.1007/s40069-016-0144-9

Fritih, Y., Vidal, T., Turatsinze, A., & Pons, G. (2013). Flexural and shear behavior of steel fiber reinforced SCC beams. *KSCE Journal of Civil Engineering, 17*(6), 1383-1393. doi: 10.1007/s12205-013-1115-1

Gencoglu, M., Komur, M., & Taskin, B. (2002). *Bending Behavior of Steel-Fiber Reinforced Concrete.* Paper presented at the Proceedings of the 4th GAP Engineering Congress.

Gensel, O., Brostow, W., Datashvili, T., & Thedford, M. (2011). Workability and Mechanical Performance of Steel Fiber-Reinforced Self-Compacting Concrete with Fly Ash. *Composite Interfaces, 18*, 169-184.

Ghavidel, R., Madandoust, R., & Ranjbar, M. M. (2015). Reliability of pull-off test for steel fiber reinforced self-compacting concrete. *Measurement, 73*, 628-639.

Goel, S., & Singh, S. (2014). Fatigue performance of plain and steel fibre reinforced self compacting concrete using S–N relationship. *Engineering Structures, 74*, 65-73. doi: 10.1016/j.engstruct.2014.05.010

Goel, S., Singh, S., & Singh, P. (2012). Flexural fatigue strength and failure probability of Self Compacting Fibre Reinforced Concrete beams. *Engineering Structures, 40*, 131-140. doi: 10.1016/j.engstruct.2012.02.035

Grünewald, S., & Walraven, J. C. (2001). Parameter-study on the influence of steel fibers and coarse aggregate content on the fresh properties of self-compacting concrete. *Cement and Concrete Research, 31*(12), 1793-1798. doi: 10.1016/s0008-8846(01)00555-5

Hassan, A., Hossain, K., & Lachemi, M. (2010). Strength, cracking and deflection performance of large-scale self-consolidating concrete beams subjected to shear failure. *Engineering Structures, 32*(5), 1262-1271. doi: 10.1016/j.engstruct.2010.01.002

Hwang, J.-H., Lee, D. H., Ju, H., Kim, K. S., Kang, T. H.-K., & Pan, Z. (2016). Shear Deformation of Steel Fiber-Reinforced Prestressed Concrete Beams. *International Journal of Concrete Structures and Materials*, 1-11. doi: 10.1007/s40069-016-0159-2

Islam, M. S., & Alam, S. (2013). Principal component and multiple regression analysis for steel fiber reinforced concrete (SFRC) beams. *International Journal of Concrete Structures and Materials, 7*(4), 303-317. doi: https://doi.org/10.1007/s40069-013-0059-7

Jabbar, S., Hejazi, F., & Mahmod, H. M. (2016). Effect of an Opening on Reinforced Concrete Hollow Beam Web Under Torsional, Flexural, and Cyclic Loadings. *Latin American Journal of Solids and Structures, 13*(8), 1576-1595. doi: https://doi.org/10.1590/1679-782512629

Kamal, M., Safan, M., Bashandy, A., & Khalil, A. (2017). Experimental Investigation on the Behavior of Normal strength and High Strength Self-Curing Self-Compacting Concrete. *Journal of Building Engineering*. doi: 10.1016/j.jobe.2017.12.012

Kamal, M. M., Safan, M. A., Etman, Z. A., & Kasem, B. M. (2014). Mechanical properties of self-compacted fiber concrete mixes. *HBRC Journal, 10*(1), 25-34. doi: 10.1016/j.hbrcj.2013.05.012

Kanellopoulos, A., Petrou, M. F., & Ioannou, I. (2012). Durability performance of self-compacting concrete. *Construction and Building Materials, 37*, 320-325. doi: 10.1680/macr.11.00165

Madandoust, R., Ranjbar, M. M., Ghavidel, R., & Shahabi, S. F. (2015). Assessment of factors influencing mechanical properties of steel fiber reinforced self-compacting concrete. *Materials & Design, 83*, 284-294. doi: 10.1016/j.matdes.2015.06.024

Mahmod, H. M., Aznieta, A. F. N., & Gatea, S. J. (2017). Evaluation of rubberized fibre mortar exposed to elevated temperature using destructive and non-destructive testing. *KSCE Journal of Civil Engineering, 21*(4), 1347-1358. doi: 10.1007/s12205-016-0721-0

Oliveira, M. J., Ribeiro, A. B., & Branco, F. G. (2015). Curing effect in the shrinkage of a lower strength self-compacting concrete. *Construction and Building Materials*. doi: 10.1016/j.conbuildmat.2015.04.035

Pająk, M., & Ponikiewski, T. (2013). Flexural behavior of self-compacting concrete reinforced with different types of steel fibers. *Construction and Building Materials, 47*, 397-408. doi: 10.1016/j.conbuildmat.2013.05.072

Sardar, S., Mahmod, M., & Shakir, I. Nonlinear Pushover Analysis for Steel Beam-Column Connection. doi: 10.23918/eajse.v3i1sip83

Shi, C., Wu, Z., Lv, K., & Wu, L. (2015). A review on mixture design methods for self-compacting concrete. *Construction and Building Materials, 84*, 387-398.

Tadepalli, P. R., Dhonde, H. B., Mo, Y., & Hsu, T. T. (2015). Shear strength of prestressed steel fiber concrete I-beams. *International Journal of Concrete Structures and Materials, 9*(3), 267-281. doi: 10.1007/s40069-015-0109-4

Tichko, S., De Schutter, G., Troch, P., Vierendeels, J., Verhoeven, R., Lesage, K., & Cauberg, N. (2015). Influence of the viscosity of self-compacting concrete and the presence of rebars on the formwork pressure while filling bottom-up. *Engineering Structures, 101*, 698-714. doi: 10.1016/j.engstruct.2015.08.008

Woo, S.-K., Kim, K.-J., & Han, S.-H. (2014). Tensile cracking constitutive model of Steel Fiber Reinforced Concrete (SFRC). *KSCE Journal of Civil Engineering, 18*(5), 1446-1454. doi: 10.1007/s12205-014-0335-3